



Preparation and application of a novel supported 3-(3-sulfamic acid imidazolium trifluoroacetate)propyl triethoxysilane on magnetic nanoparticles as a new magnetic ionic liquid for the synthesis of triazole quinazolinones and fused pyrimidines

Narjes Basirat¹

Received: 17 March 2020 / Accepted: 12 September 2020
© Springer Nature B.V. 2020

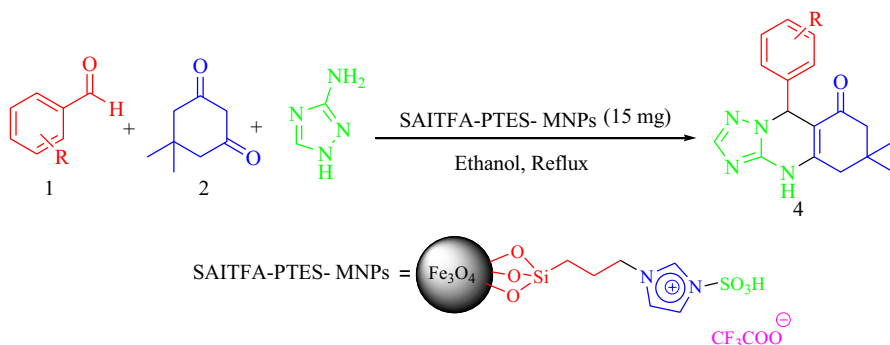
Abstract

Supported 3-(3-sulfamic acid imidazolium trifluoroacetate)propyl triethoxysilane on magnetic nanoparticles as a novel nanocatalyst was synthesized and characterized by FT-IR, XRD, TGA, SEM, TEM and VSM techniques. The catalytic activity of the magnetic catalyst was studied through one-pot synthesis of triazole quinazolinones and fused pyrimidine derivatives via one-pot multi-component reactions under thermal conditions. This catalyst demonstrated excellent catalytic properties with high percentage in short reaction times, low cost and easily separated using an external magnet and reusable without significant loss of its catalytic efficiency.

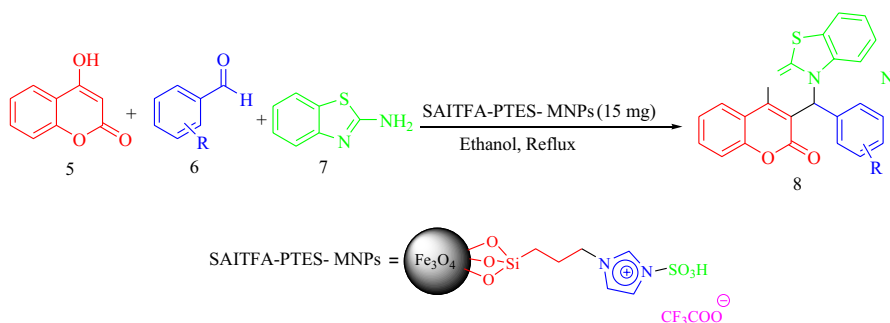
Electronic supplementary material The online version of this article (<https://doi.org/10.1007/s11164-020-04271-z>) contains supplementary material, which is available to authorized users.

✉ Narjes Basirat
kimiabasirat51@gmail.com

¹ Department of Chemistry, Payame Noor University (PNU), Tehran, Iran



Scheme 1 Synthesis of triazole quinazolinone derivatives by in the presence of TFA-SAI-PTES-MNPs as a nanomagnetic catalyst



Scheme 2 Synthesis of fused pyrimidine derivatives using TFA-SAI-PTES-MNPs nanoparticle as a nanomagnetic catalyst

for synthesis of triazole quinazolinone and fused pyrimidine derivatives via MCRs, such as $H_6P_2W_{18}O_{62} \cdot 18H_2O$ [24], molecular iodine [25], acetic acid [26], ionic liquids [27], sodium lauryl sulphate (SLS) micelles [28] and hydrotalcite [29].

In this paper, we synthesized a novel supported 3-(3-sulfamic acid imidazolium trifluoroacetate)propyl triethoxysilane on magnetic nanoparticles (TFA-SAI-PTES-MNPs) as a new magnetic ionic liquid and inspected its catalytic application for synthesis of triazole quinazolinone derivatives from three component reactions of aldehyde, dimedone, 3-amino-1,2,4-triazole and preparation of fused pyrimidines derivatives from three component reactions of 4-hydroxycoumarin, arylaldehyde and 2-aminobenzothiazole via one-pot multi-component reactions (Scheme 1 and 2).

Chemicals and materials

An Electrothermal 9100 device was used for measuring melting points. In order to characterize desired catalyst, X-ray diffraction (XRD) pattern was recorded on a Philips PW 1830 X-ray diffractometer with $CuK\alpha$ source ($\lambda = 1.5418 \text{ \AA}$) at $25 \text{ }^\circ\text{C}$ temperature.

The morphology of the catalyst was tested using scanning electron microscopy model VEGA//TESCAN KYKY-EM 3200 in acceleration voltage 26 kV. Fourier transform infrared (FT-IR) spectrum was recorded with a FT-IR Bruker vector 22 spectrophotometer at room temperature in the range of 400–4000 cm^{-1} . Transmission electron microscopy (TEM) catalyst was performed on a Philips EM 208 electron microscope. Magnetic measurements were taken using vibration sample magnetometer (VSM, MDK and Model 7400). Bruker DRX-400 AVANCE instrument (300 MHz for ^1H , 75.5 MHz for ^{13}C) was used for recording of NMR spectra using CDCl_3 as solvent.

General procedure

Preparation of the magnetic Fe_3O_4 nanoparticles (MNPs)

$\text{FeCl}_3 \cdot 6\text{H}_2\text{O}$ (4.865 g, 0.018 mol) and $\text{FeCl}_2 \cdot 4\text{H}_2\text{O}$ (1.789 g, 0.0089 mol) were added to 100 ml deionized water and sonicated until the salts dissolved completely. Then, 10 ml of 25% NH_4OH (10 ml) was added quickly into the reaction mixture in one portion under N_2 atmosphere at room temperature, followed by stirring about 30 min with mechanical stirrer. The black precipitate was washed with doubly distilled water (five times) (Scheme 3).

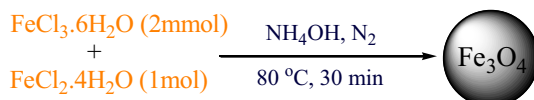
Preparation of 3-chloropropyl triethoxysilane functionalized Fe_3O_4 nanoparticles (CPTES-MNPs)

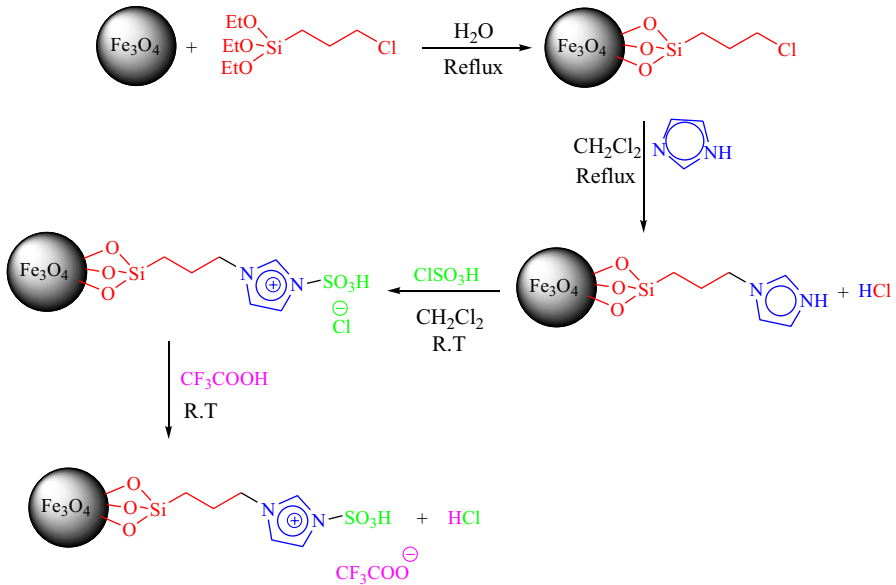
The obtained MNPs powder (1 g) was dispersed in 150 ml water solution by sonication for 30 min, and then, 2.5 ml of CPTES was added to the above mixture in which a black suspension was formed. This suspension was then refluxed at 100 $^\circ\text{C}$ for 6 h, with vigorous stirring. CPTES-MNPs nanoparticle was separated from the aqueous solution by magnetic decantation, washed with distilled water several times and then dried in an oven overnight (Scheme 4). Whole synthesis was done under N_2 atmosphere.

Preparation of imidazole supported on CPTES-MNPs nanoparticles (I-PTES-MNPs)

The obtained CPTES-MNPs powder (1 g) was dispersed in CH_2Cl_2 (50 ml) solution by sonication for 30 min, and then, 1 g imidazole was added to the above mixture in which a black suspension was formed. This suspension was then refluxed for 12 h, with vigorous stirring. HCl gas expelled from the reaction. I-PTES-MNPs nanoparticle was separated from the aqueous solution by magnetic decantation, washed with distilled water several times and then dried in an oven overnight (Scheme 4). Whole synthesis was done under N_2 atmosphere.

Scheme 3 Preparation of Fe_3O_4 nanoparticles





Scheme 4 Preparation of TFA-SAI-PTES-MNPs nanoparticles

Preparation of 3-(3-sulfamic acid imidazolium chloride)propyl triethoxysilane functionalized Fe_3O_4 nanoparticles (CSAI-PTES-MNPs)

The I-PTES-MNPs (0.75 g) were dispersed in dry CH_2Cl_2 (10 ml) by ultrasonic bath for 30 min. Eventually, chlorosulfuric acid (0.7 ml) was added dropwise over a period of 25 min at room temperature. Hydrogen gas expelled from the reaction. Then, the prepared functionalized MNPs nanoparticles were separated by magnetic field and washed with dry CH_2Cl_2 four times to remove the unattached substrates (Scheme 4).

Preparation of 3-(3-sulfamic acid imidazolium fluoroacetate)propyl triethoxysilane functionalized Fe_3O_4 nanoparticles (TFA-SAI-PTES-MNPs)

The CSAI-PTES-MNPs (0.5 g) was dispersed in dry CH_2Cl_2 (10 ml) by ultrasonic bath for 30 min. Eventually, trifluoroacetic acid (1 ml) was added dropwise over a period of 30 min at room temperature. Hydrogen chloride was produced in the reaction and expelled from the reaction. Then, the prepared functionalized MNPs nanoparticles was separated by magnetic field and washed with dry CH_2Cl_2 four times to remove the unattached substrates (Scheme 4).

General procedure for the synthesis of triazole quinazolinone derivatives by TFA-SAI-PTES-MNPs nanoparticles as a new ionic liquid nanocatalyst

For the synthesis of the triazole quinazolinone derivatives, the reaction of aldehyde **1** (1 mmol), dimedone **2** (1 mmol) and 3-amino-1,2,4-triazole **3** (1 mmol) was performed at the presence of TFA-SAI-PTES-MNPs (15 mg) as ionic liquid nanomagnetic catalyst with vigorous stirring in ethanol solvent under reflux conditions for the appropriate time. After completion of the reaction, checked by TLC, the catalyst was separated using an external magnet for separation of the catalyst, checking the reusability. The solution containing the product was evaporated to give the solid. The solid was recrystallized with ethanol to give the pure solid. All desired products were characterized by comparison of their physical data with those of known compounds.

Selected spectra for three known and reported products are provided below

6,7-Dihydro-9-phenyl-6,6-dimethyl-[1,2,4]triazolo[5,1-b]quinazolin-8(4H,5H,9H)-one (**4a**): white powder; yield (95%); mp=245–247 °C.; IR (KBr): ν_{\max} =3369–3000, 2955, 2925, 1715, 1657, 1615, 1459 cm^{-1} .; ^1H NMR (400 MHz, DMSO- d_6): δ =11.06 (1H, s, NH), 7.80 (1H, s, Ar), 7.05–7.17 (5H, m, Ar), 6.05 (1H, s, CH), 2, m.63–2.71 (2H, CH₂), 2.21 (1H, d, J=8.3 Hz, CH₂), 2.12 (1H, d, J=8.3 Hz, CH₂), 1.13 (3H, s, CH₃), 0.92 (3H, s, CH₃) ppm.; ^{13}C NMR(100 MHz, DMSO- d_6): δ =192.1 (C=O), 154.5 (C=N), 149.3 (C=N), 145.0 (CH_{Ar}), 142.1 (CH_{Ar}), 130.8 (CH_{Ar}), 128.3 (CH_{Ar}), 108.2 (C-N), 57.4 (CH), 51.3 (CH₂), 48.5 (CH₂), 29.3 (CH₃), 25.0 (CH₃) ppm.

6,7-Dihydro-6,6-dimethyl-9-p-tolyl-[1,2,4]triazolo[5,1-b]quinazolin-8(4H,5H,9H)-one (**4b**): Yellow powder; Yield (94%); mp=260–263 °C. IR (KBr): ν_{\max} =3380–3022, 2957, 2922, 1711, 1610, 1461 cm^{-1} .; ^1H NMR (400 MHz, DMSO- d_6): δ =11.05 (1H, s, NH), 7.70 (1H, s, Ar), 7.03 (4H, s, Ar), 7.03 (4H, s, Ar), 6.09 (1H, s, CH), 2.62–2.70 (2H, m, CH₂), 2.38 (1H, s, CH₃), 2.24 (1H, d, J=5.7 Hz, CH₂), 2.17 (1H, d, J=5.7 Hz, CH₂), 1.11 (3H, s, CH₃), 0.98 (3H, s, CH₃) ppm.; ^{13}C NMR(100 MHz, DMSO- d_6): δ =192.9 (C=O), 154.5 (C=N), 149.0 (C=N), 144.1 (CH_{Ar}), 143.6 (CH_{Ar}), 129.9 (CH_{Ar}), 128.6 (CH_{Ar}), 126.0 (CH_{Ar}), 108.1 (C-N), 57.2 (CH), 51.6 (CH₂), 48.5(CH₂), 29.2 (CH₃), 24.8(CH₃), 22.3(CH₃) ppm.

6,7-Dihydro-9-phenyl-6,6-dimethyl-[1,2,4]triazolo[5,1-b]quinazolin-8(4H,5H,9H)-one (**4e**): white powder; yield (98%); IR (KBr): ν_{\max} =3352–3003, 2961, 2927, 1710, 1654, 1612, 1442, 1112 cm^{-1} .;mp=299–300 °C.; ^1H NMR (400 MHz, DMSO- d_6): δ =11.20 (1H, s, NH), 7.28 (1H, s, Ar), 7.44 (2H, d, J=7.4, Ar), 7.35 (2H, d, J=7.4, Ar), 6.20 (1H, s, CH), 2.31–2.40 (2H, m, CH₂), 2.20 (1H, d, J=6 Hz, CH₂), 2.00 (1H, d, J=6 Hz, CH₂), 1.14 (3H, s, CH₃), 0.90 (3H,

s, CH₃) ppm.; ¹³C NMR(100 MHz, DMSO-*d*₆): δ = 190.2(C=O), 155.4(C=N), 149.0(C=N), 146.3(CH_{Ar}), 142.2(CH_{Ar}), 135.3(CH_{Ar}), 130.2(CH_{Ar}), 128.0(CH_{Ar}), 111.9(C-N), 50.1(CH), 48.5(CH₂), 47.1(CH₂), 26.1(CH₃), 25.7(CH₃) ppm.

General procedure for the synthesis of fused pyrimidines by TFA-SAI-PTES-MNPs as a new ionic liquid nanocatalyst

The mixture of 4-hydroxycomarin **5** (1 mmol), arylaldehydes **6** (1 mmol), 2-aminobenzothiazole **7** (1 mmol) and 20 mg TFA-SAI-PTES-MNPs as ionic liquid nanomagnetic catalyst in ethanol solvent under reflux conditions for the specific times. After completion of the reaction, checked by TLC, the catalyst was separated by using an external magnet for separation of the catalyst and checking the reusability. The solution containing the product was evaporated to give the solid. The solid was recrystallized with ethanol to give the pure solid. All desired products were characterized by comparison of their physical data with those of known compounds.

Selected spectra for three known and reported products are provided below

7-phenylchromeno[4,3-*d*]benzothiazolo[3,2-*a*]pyrimidin-6(7H)-one (**8a**): white powder; yield (94%); mp = 200–201 °C.; IR (KBr): ν_{\max} = 2955, 2892, 1690, 1602, 1459, 1120 cm⁻¹.; ¹H NMR (400 MHz, DMSO-*d*₆): δ = 7.36–7.47 (4H, m, Ar), 7.17–7.24 (5H, m, Ar), 7.00–7.06 (4H, m, Ar), 6.27 (1H, s, CH) ppm.; ¹³C NMR(100 MHz, DMSO-*d*₆): δ = 170.3(C=O), 168.8 (C=C), 164.8(C=C), 160.8(C=C), 146.3, 145.6, 135.6, 134.5, 133.8, 131.2, 130.4, 128.8, 127.6, 126.5, 123.8, 122.5, 117.8, 117.5, 116.3 (C-N), 105.8 (C-S), 88.5(CH) ppm.

7-(4-nitrophenyl)chromeno[4,3-*d*]benzothiazolo[3,2-*a*]pyrimidin-6(7H)-one (**8i**): white powder; yield (93%); mp = 292–295 °C.; IR (KBr): ν_{\max} = 2990, 2900, 1700, 1602, 1550, 1459, 1362, 1119 cm⁻¹.; ¹H NMR (400 MHz, DMSO-*d*₆): δ = 8.17 (2 H, d, J = 6.7, Ar), 7.78 (2 H, d, J = 6.4, Ar), 7.52 (2H, t, J = 5.8, Ar), 7.33 (2H, q, J = 5.8, Ar), 7.20–7.25 (4H, m, Ar), 6.14 (1H, s, CH) ppm.; ¹³C NMR(100 MHz, DMSO-*d*₆): δ = 170.4 (C=O), 168.1 (C=C), 163.6 (C=C), 156.0 (C=C), 144.8, 135.9, 133.0, 132.6, 129.6, 129.4, 128.8, 128.3, 127.6, 127.3, 127.1, 125.2, 123.3, 121.9, 121.2 (C-N), 107.2 (C-S), 82.4(CH) ppm.

7-(4-chlorophenyl)chromeno[4,3-*d*]benzothiazolo[3,2-*a*]pyrimidin-6(7H)-one (**8l**): white powder; yield (93%); mp = 194–197 °C.; IR (KBr): ν_{\max} = 2962, 2872, 1691, 1611, 1459, 1110 cm⁻¹.; ¹H NMR (400 MHz, DMSO-*d*₆): δ = 7.86 (2 H, d, J = 9.5, Ar), 7.77 (2 H, d, J = 9.5, Ar), 7.42–7.48 (4H, m, Ar), 7.29 (1H, t, J = 6.0, Ar), 7.19 (1 H, d, J = 6.7, Ar), 7.06–7.10 (2H, m, Ar), 6.33 (1H, s, CH) ppm.; ¹³C NMR(100 MHz, DMSO-*d*₆): δ = 172.6 (C=O), 168.8 (C=C), 163.4 (C=C), 159.6 (C=C), 145.7, 144.1, 136.8, 136.0, 135.2, 133.3, 130.5, 129.7, 129.0, 128.7, 127.6, 126.5, 125.6, 112.1 (C-N), 104.6 (C-S), 81.9 (CH) ppm.

Results and discussion

Characterization of the synthesized TFA-SAI-PTES-MNPs ionic liquid magnetic nanoparticle

X-ray diffraction (XRD) analysis

X-ray diffraction was used to identify the crystal-line structure of synthesized TFA-SAI-PTES-MNPs magnetic nanoparticle. The X-ray diffraction pattern was observed and found that standard Fe_3O_4 crystal has six diffraction peaks, i.e., (220), (311), (400), (422), (511) and (440) at $2\theta = 30, 35.5, 43.5, 54, 57, 63$ (Fig. 1). The average TFA-SAI-PTES-MNPs magnetic nanoparticle diameter was calculated to be approximately 15 nm from the XRD results by Scherrer's equation, $D = k\lambda/\beta\cos\theta$, where k is a constant (generally considered as 0.94), λ is the wavelength of Cu K α (1.54 Å), β is the corrected diffraction line full-width at half-maximum (FWHM), and θ is Bragg's angle [30, 31].

Fourier transforms infrared (FT-IR) analysis

FT-IR spectrum of the TFA-SAI-PTES-MNPs magnetic nanoparticle is shown in Fig. 2. The peaks at 585 and 448 cm^{-1} were resulted from Fe-O stretching band and 3426 cm^{-1} corresponded to broad OH groups on magnetic surface of MNPs. The peaks at 2855 and 2924 cm^{-1} are the characteristic bands contributing to the symmetric and asymmetric stretching of C-H bond in imidazolium fluoroacetate and propyl group unit of TFA-SAI-PTES-MNPs magnetic nanoparticle. The vibration band occurred at 1635 cm^{-1} represented the $-\text{C}=\text{O}$ functional group. The peaks at 1180 and 1116 cm^{-1} are due to the sulfonyl groups. Also, adsorption bands at 1044 cm^{-1} are due to the Si-O groups. So, here, FT-IR spectrum confirms prepared catalyst structure.

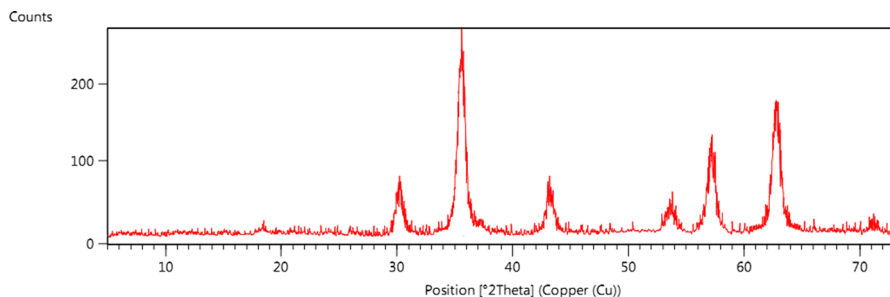


Fig. 1 XRD pattern of TFA-SAI-PTES-MNPs magnetic nanoparticle

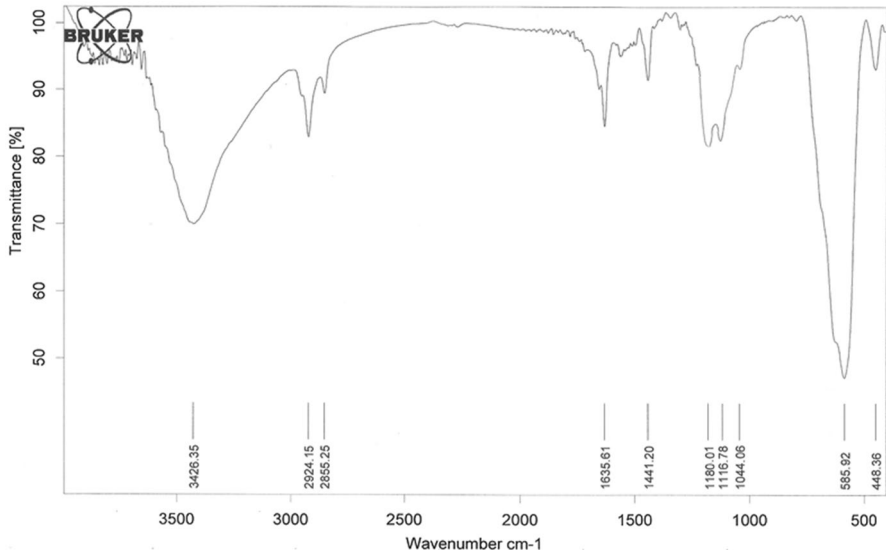


Fig. 2 FT-IR spectrum of the TFA-SAI-PTES-MNPs magnetic nanoparticle

Thermogravimetric analysis (TGA)

Information about loading of magnetic nanoparticles with organic group is obtained by thermogravimetric analysis (TGA). The results revealed that the TFA-SAI-PTES-MNPs nanoparticles contain about 13% of organic moieties (volatile components disappearing until a temperature of about 100 °C are neglected) (Fig. 3). The mass weight loss about 6.2% between 100 and 300 °C is contributed to the thermal decomposition of the sulfamic acid and fluoroacetate groups. The mass weight loss of 6.8% between 300 and 860 °C is related to the breakdown of the 3-imidazolepropyl silane group. It is concluded that the well grafting of 3-(3-sulfamic acid imidazolium fluoroacetate)propyl triethoxysilane on the Fe_3O_4 nanoparticles is confirmed.

TEM analysis

Morphology of synthesized TFA-SAI-PTES-MNPs magnetic nanoparticle was Survey by TEM that shown in Fig. 4. The average size of nanoparticle circa 16 nm from the TEM micrographs is in very good settlement with the crystallite size computed from XRD at 15 nm.

Scanning electron microscope (SEM)

Scanning electron microscopy (SEM) is known as a primary tool for determining the size distribution, surface morphology, particle shape and structural properties.

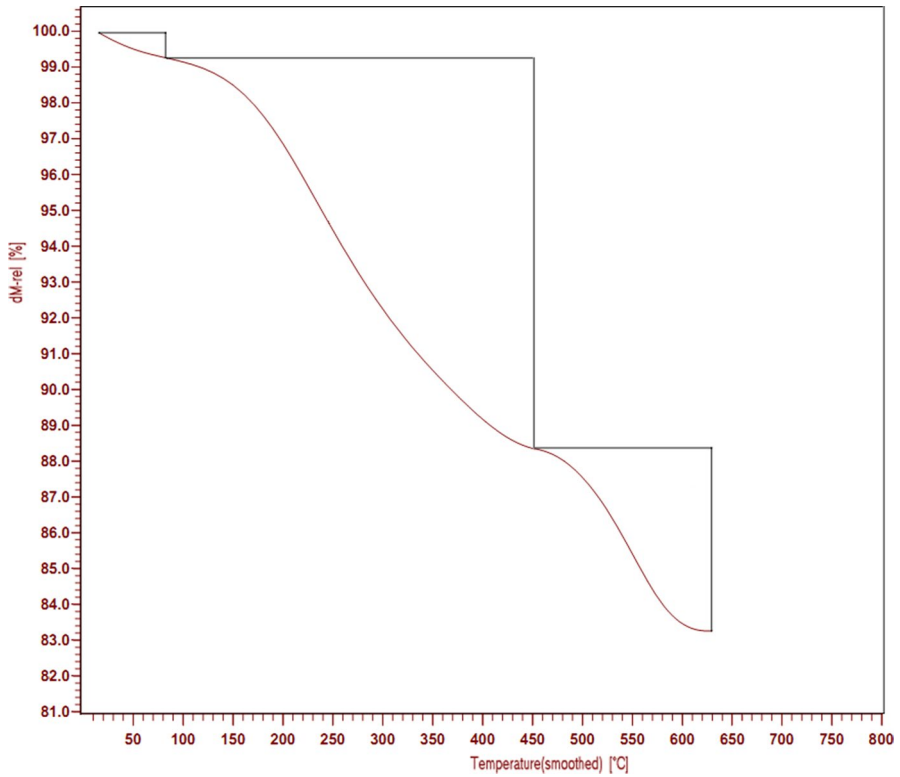


Fig. 3 Thermogravimetric analysis of TFA-SAI-PTES-MNPs magnetic nanoparticles

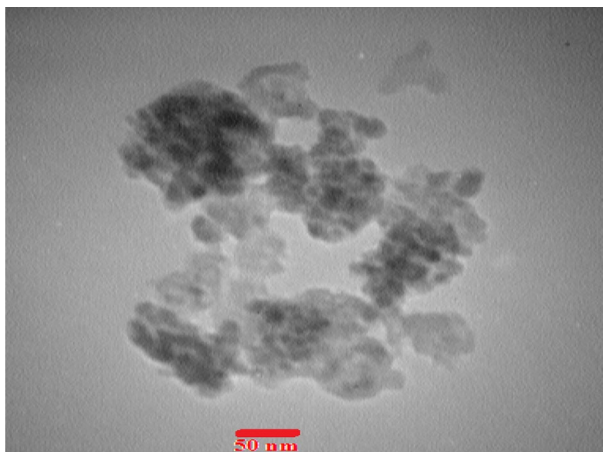


Fig. 4 TEM micrographs of magnetic TFA-SAI-PTES-MNPs

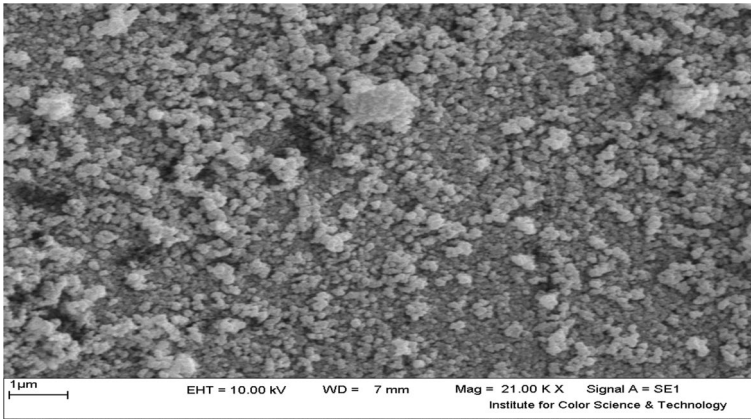


Fig. 5 The SEM image of TFA-SAI-PTES-MNPs magnetic nanoparticle

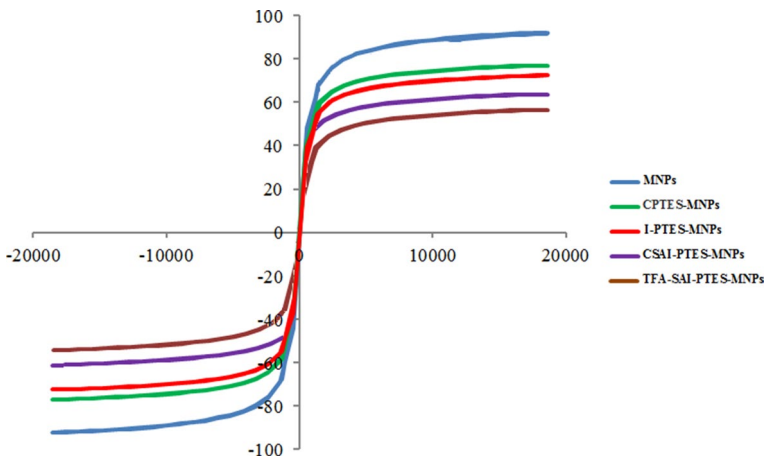


Fig. 6 Room-temperature magnetization curves of MNPs, CPTES-MNPs, I-PTES-MNPs, CSAI-PTES-MNPs and TFA-SAI-PTES-MNPs magnetic nanoparticle

The SEM image of the TFA-SAI-PTES-MNPs magnetic nanoparticle is presented in Fig. 5. According to this image, size distribution is narrow and the mean size of the nanomagnetic catalyst is about 15–30 nm.

Vibrating sample magnetometer (VSM)

Curves related to magnetic properties of the nanoparticles of MNPs, CPTES-MNPs, I-PTES-MNPs, CSAI-PTES-MNPs and TFA-SAI-PTES-MNPs are shown in Fig. 6. Saturation magnetization of nanoparticles of MNPs, CPTES-MNPs, I-PTES-MNPs, CSAI-PTES-MNPs and TFA-SAI-PTES-MNPs was about 91.6, 76.8, 72.3, 64.3 and 57.6 emu/g, respectively. As can be observed, there is a decrease in magnetic

property which confirmed the adhering of functional groups to nanoparticles. Decrease in magnetic property in TFA-SAI-PTES-MNPs than MNPs affirms adhering of 3-(3-sulfamic acid imidazolium fluoroacetate)propyl triethoxysilane group to this nanoparticle.

Catalytic application of TFA-SAI-PTES-MNPs magnetic nanocatalyst

First, to optimize the amounts of the catalyst and reactions conditions, the solvent-free reaction of benzaldehyde (1 mmol), dimedone (1 mmol) and 3-amino-1,2,4-triazole (1 mmol) in the presence of different amount of TFA-SAI-PTES-MNPs as catalyst in ethanol was examined. The reaction was carried out with 10, 15 and 20 mg of at room temperature, 50 °C and reflux (Table 1). As shown from Table 1, 15 mg of TFA-SAI-PTES-MNPs at reflux conditions afforded 9-phenyl-6,6-dimethyl-5,6,7,9-tetrahydro-4H-1,2,4-triazolo[5,1-b]quinazolin-8-one in 18 min with 95% of yield (Table 1, entry 8).

In the following, three-component condensation reaction of the aromatic aldehydes **1**, dimedone **2** and 3-amino-1,2,4-triazole **3**, under optimum conditions for the synthesis of the triazole quinazolinone derivatives, was studied. The wide ranges of substituted different aldehydes with their corresponding products were synthesized in good to high yields using the TFA-SAI-PTES-MNPs as magnetic nanocatalyst. The presence of electron donating groups on the aromatic aldehydes afforded the corresponding products in moderate yields, and the reaction was sluggish; however, the presence of electron-withdrawing groups afforded the corresponding products in shorter reaction times with higher yield (Table 2).

The proposed mechanism for the reaction using TFA-SAI-PTES-MNPs is described for the preparation of **4a** from benzaldehyde **1**, dimedone **2** and 3-amino-1,2,4-triazole **3** in Scheme 2. According to the literature report [27, 32, 33], 2-benzylidene-5,5-dimethylcyclohexane-1,3-dione (**I**), containing the electron-poor C=C double bond, is formed quantitatively by Knoevenagel addition of dimedone **2** to the benzaldehyde **1** in the presence of TFA-SAI-PTES-MNPs as magnetic nanocatalyst and then subsequent Michael-type addition of 3-amino-1,2,4-triazole **3** to

Table 1 Effect of different amounts of TFA-SAI-PTES-MNPs as catalyst and various temperatures on the reaction benzaldehyde (1 mmol), dimedone (1 mmol) and 3-amino-1,2,4-triazole (1 mmol) in ethanol solvent

Entry	Catalyst (mol%)	Temperature (°C)	Time (min)	Yield (%) ^a
1	10	25	60	Trace
2	15	25	60	Trace
3	20	25	60	15
4	10	50	45	37
5	15	50	40	45
6	20	50	36	52
7	10	Reflux	20	80
8	15	Reflux	14	96
9	20	Reflux	14	97

^aIsolated yield

Table 2 Synthesis of triazole quinazolinones in the presence of TFA-SAI-PTES-MNPs as magnetic nanocatalyst

Entry	Aldehydes	Products	Time(min)	Yield ^a (%)	MP(°C)	
					Found	Reported
1	C ₆ H ₅	4a	14	95	245–247	248–250 [27]
2	4-MeC ₆ H ₄	4b	17	94	260–263	264–269 [27]
3	4-OMeC ₆ H ₄	4c	22	93	295–297	>300 [32]
4	4-NO ₂ C ₆ H ₄	4d	9	97	293–295	>300 [32]
5	4-ClC ₆ H ₄	4e	10	98	299–300	307–309 [25]
6	4-OHC ₆ H ₄	4f	27	92	298–300	304–306 [26]
7	3-NO ₂ C ₆ H ₄	4g	13	96	260–263	266–269 [33]

^aIsolated yield

intermediate (II). Tautomerization converts intermediate (II) to intermediate (III). After that, the intermediate (III) was cyclized by the nucleophilic attack of NH group on the C=O moiety and gave the intermediate (IV). Then, the elimination of water gave their corresponding product **4a** (Scheme 5).

We also investigated recycling of the TFA-SAI-PTES-MNPs as ionic liquid nano-magnetic catalyst under ethanol solvent at reflux conditions using the model reaction of benzaldehyde **1**, dimedone **2** and 3-amino-1,2,4-triazole (Table 2, entry 4). After completion of the reaction, the catalyst was separated by using an external magnet for separation of the catalyst and checking the reusability for subsequent experiments to check their reusability under similar reaction conditions. The results showed that TFA-SAI-PTES-MNPs are a stable catalyst in reaction media and can be reused several times without significant loss of catalytic activity (Figs. 7 and 8).

To exhibit the availability and applicability of the presented work, it can be compared with several reported results in the other literature. The results demonstrated

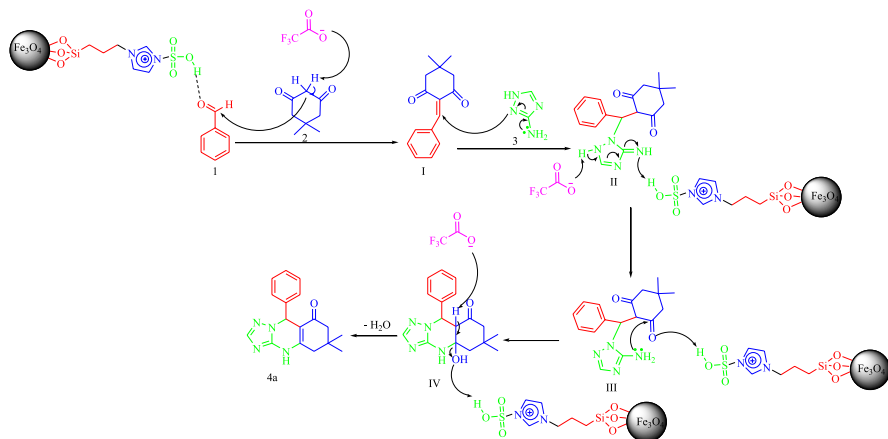
**Scheme 5** The proposed mechanism for the preparation of **4a**



Fig. 7 Image shows that TFA-SAI-PTES-MNPs as magnetic nanocatalyst can be separated by using magnetic field. A reaction mixture in the absence (right) or presence of a magnetic field (left)

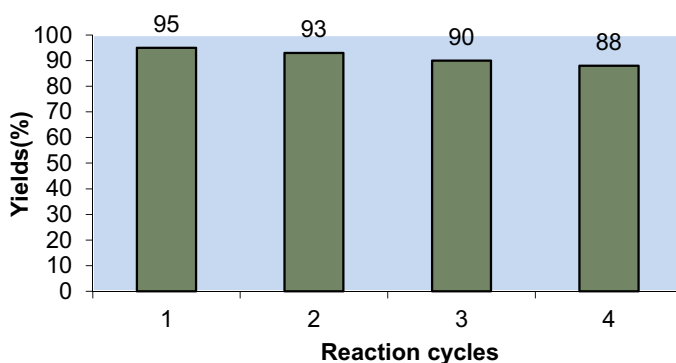


Fig. 8 The recycling of the TFA-SAI-PTES-MNPs as magnetic nanocatalyst

Table 3 Comparison of the results of TFA-SAI-PTES-MNPs with other catalysts in the synthesis of compound **4a**

Entry	Catalyst	Conditions	Time (min)	Yield(%) ^a [Ref]
1	Iodine (10 mol%)	CH ₃ CN, reflux	10	84 [25]
2	acetic acid (5 ml)	60 °C	25	95 [32]
3	NH ₂ SO ₃ H(0.05 mmol)	CH ₃ CN(5 ml), 80 °C	30	95 [33]
4	TFA-SAI-PTES-MNPs (15 mg)	Ethanol, reflux	14	96(Present work)

^aYields refer to isolated pure products

which the reactions were performed in low times and excellent yield in the presence of TFA-SAI-PTES-MNPs than other catalysts with the same yields (Table 3).

Following, it synthesized fused pyrimidine derivatives with the TFA-SAI-PTES-MNPs catalyst. For this purpose, at first, it optimized the amounts of the catalyst and reactions conditions, the solvent-free reaction of 4-hydroxycomarin (1 mmol), 4-methoxybenzaldehyde (1 mmol), 2-aminobenzothiazole (1 mmol) and ethanol solvent in the presence of different amount of TFA-SAI-PTES-MNPs

Table 4 Effect of different amounts of TFA-SAI-PTES-MNPs nanocatalyst and various temperatures on the reaction of 4-hydroxycomarin (1 mmol), 4-methoxybenzaldehyde (1 mmol) and 2-aminobenzothiazole in ethanol solvent conditions

Entry	Cata-lyst (mol%)	Temperature (°C)	Time (h)	Yield ^a (%)
1	10	25	10	Trace
2	20	25	10	Trace
3	30	25	10	24
4	10	50	6	50
5	20	50	5	59
6	30	50	4.5	67
7	10	Reflux	2.5	81
8	20	Reflux	2	94
9	30	Reflux	2	95

^aIsolated yield**Table 5** Synthesis of fused pyrimidine derivatives in the presence of TFA-SAI-PTES-MNPs as magnetic nanocatalyst in ethanol at reflux conditions

Entry	Aldehydes	Products	Time (min)	Yield (%) ^a	MP (°C)	
					Found	Reported
1	H	8 a	2	94	200–201	200–202 [29]
2	4-OEt	8b	2	93	262–264	264–267 [29]
3	4-OMe	8c	2.5	94	231–235	236–239 [29]
4	3-OMe	8d	2.5	94	245–248	249–252 [29]
5	2-Cl	8e	2	93	229–231	232–235 [28]
6	2-Br	8f	2	92	213–216	216–219 [28]
7	4-Me	8g	2.5	93	248–251	248–251 [28]
8	4-OH	8h	2.5	92	278–281	281–282 [28]
9	4-NO ₂	8i	2	93	292–295	296–298 [28]
10	3-NO ₂	8j	2.5	90	262–266	266–269 [28]
11	4-CN	8k	2.5	91	265–267	268–272 [28]
12	4-Cl	8l	2	93	194–197	198–202 [28]
13	4-Br	8m	2.5	93	241–244	247–250 [28]

^aisolated yield

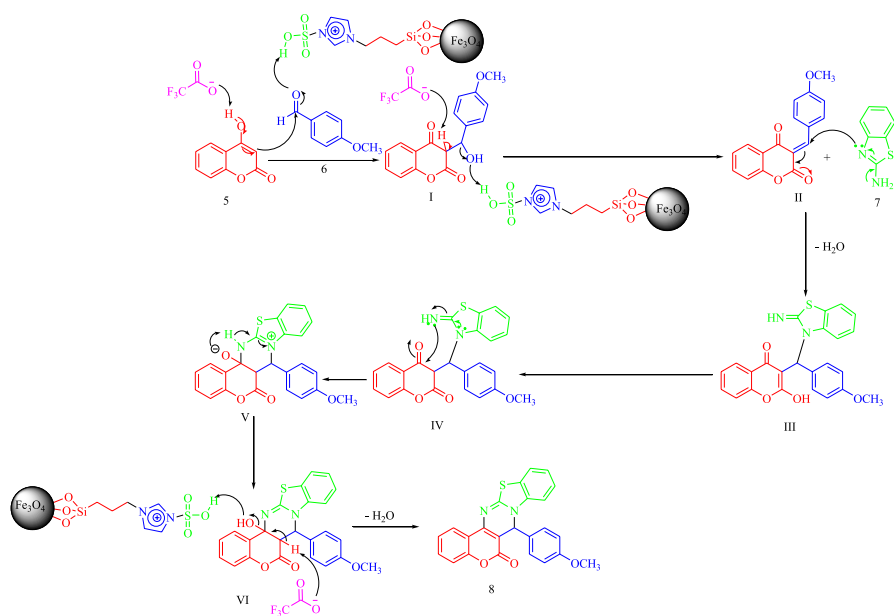
as ionic liquid nanomagnetic catalyst. The reaction was carried out with 10, 20 and 30 mg of at different temperature (25 °C, 50 °C and reflux) conditions (Table 4). As it was shown from Table 2, 20 mg of TFA-SAI-PTES-MNPs in ethanol at reflux conditions afforded 7-(4-methoxyphenyl)chromeno[4,3-d]benzothiazolo[3,2-a]pyrimidin-6(7H)-one in 2 h with 94% of yield (Table 4, entry 8).

Next, the substrate scope of the reaction was then evaluated using a variety of structurally diverse aldehydes. As shown in Table 5, the reactions with the aromatic aldehydes including electron-donating or electron-withdrawing substituents afforded the desired products in high to excellent yields (Table 5).

According to literature reported [29], in the beginning, mechanism involves the Knoevenagel condensation of the 4-hydroxycoumarin **5** and 4-methoxy benzaldehyde **6** in the presence of TFA-SAI-PTES-MNPs as nanocatalyst to giving intermediate (I). The basic sites of the catalyst abstract an acidic proton of hydroxyl group, and then, subsequent attack on the carbonyl group furnishes condensed product. This is followed by Michael addition of 2-aminobenzothiazole (3) to the C=C bond of intermediate (II) and form intermediate (III) through tautomerization. Then, an intramolecular cyclic condensation of the amino and the carbonyl groups of the Michael adduct (III) occurs to afford intermediate (IV), which afford the desired compounds (**8**) on dehydration (Scheme 6).

The recycling of the TFA-SAI-PTES-MNPs as nanocatalyst was studied using the model reaction 4-hydroxycoumarin, 4-methoxybenzaldehyde and 2-aminobenzothiazole in ethanol solvent at reflux conditions (Table 2, Entry 3) (Experimental section). The recovered catalyst was reused four runs without any loss of its activities (Fig. 9).

In order to show the accessibility of the present work, it was compared with other reported results in the literature in Table 6. The results show that the reaction in the presence of TFA-SAI-PTES-MNPs as ionic liquid nanomagnetic catalyst was carried out in short times and high yields (Table 6).



Scheme 6 The proposed mechanism for the preparation of **8c** in the presence of TFA-SAI-PTES-MNPs as nanocatalyst

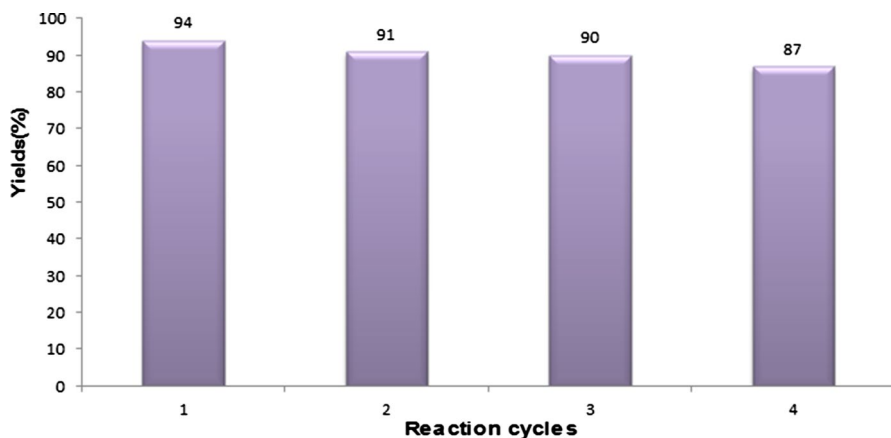


Fig. 9 The recycling of the TFA-SAI-PTES-MNPs in the reaction of 4-hydroxycoumarin, 4-methoxybenzaldehyde and 2-aminobenzothiazole

Table 6 Comparison the results of TFA-SAI-PTES-MNPs with other catalysts in the synthesis of compound **8a**

Entry	Catalyst	Conditions	Time (h)	Yield(%) ^a [Ref]
1	sodium lauryl sulphate (SLS) (10 mol%)	water(10 ml), r.t	5	95 [28]
2	hydrotalcite (100 mg)	70 °C, solvent-free	2	95 [29]
3	TFA-SAI-PTES-MNPs (20 mg)	Ethanol, reflux	2	94

(Present work)

^aYields refer to isolated pure products

Conclusions

We synthesized TFA-SAI-PTES-MNPs as an ionic liquid nanomagnetic catalyst characterized by XRD, EXD, FT-IR, TEM, SEM and VSM techniques. Size evaluation via various techniques shows the size of TFA-SAI-PTES-MNPs magnetic nanocatalyst around 26–37 nm. The most interesting features of the this work include stability as well as efficient catalytic activity for synthesis of triazole quinazolinones and fused pyrimidines derivatives via one-pot multi-component reactions under thermal conditions. The attractive features of this procedure are simple process, inexpensive work up, ease of handling, high yields of products and use of recyclable nanomagnetic catalyst.

Acknowledgements This research was supported by the Research Council of the Payame Noor University (PNU) in Iran.

References

1. C. Bréchnignac, P. Houdy, M. Lahmani, *Nanomaterials and nanochemistry* (Springer Science and Business Media, Berlin, 2008)
2. V. Pokropivny, R. Lohmus, I. Hussainova, A. Pokropivny, S. Vlassov, *Introduction to nanomaterials and nanotechnology* (Tartu University Press, Ukraine, 2007)
3. K. Sobolev, I. Flores, R. Hermosillo, L.M. Torres-Martínez, In Proceedings of ACI Session on “Nanotechnology of Concrete: Recent Developments and Future Perspectives”, (2006)
4. S. Laurent, D. Forge, M. Port, A. Roch, C. Robic, L. Vander Elst, R.N. Muller, *Chem Rev* **108**, 2064 (2008)
5. S. Asghari, M. Mohammadnia, *Res Chem Intermed* **42**, 1899 (2016)
6. W. Wu, Q. He, C. Jiang, *Nanoscale Res Lett* **3**, 397 (2008)
7. S. Asghari, M. Mohammadnia, *Res Chem Intermed* **43**, 7193 (2017)
8. A.K. Gupta, M. Gupta, *Biomaterials* **26**, 3995 (2005)
9. E. Amstad, S. Zurcher, A. Mashaghi, J.Y. Wong, M. Textor, E. Reimhult, *Small* **5**, 1334 (2009)
10. S. Asghari, M. Mohammadnia, *Inorg Nano-met Chem* **47**, 1004 (2017)
11. N.A. Frey, S. Peng, K. Cheng, S. Sun, *Chem Soc Rev* **38**, 2532 (2009)
12. J. Chomoucka, J. Drbohlavova, D. Huska, V. Adam, R. Kizek, J. Hubalek, *Pharmacol Res* **62**, 144 (2010)
13. H.R. Shaterian, M. Mohammadnia, *Res Chem Intermed* **40**, 371 (2014)
14. C. Hulme, V. Gore, *Curr Med Chem* **10**, 51 (2003)
15. D.B. Ramachary, M. Kishor, G.B. Reddy, *Org Biomol Chem* **4**, 1641 (2006)
16. A. Kumar, S. Sharma, R.A. Maurya, *Tetrahedron Lett* **50**, 5937 (2009)
17. W. Yu, C. Goddard, E. Clearfield, C. Mills, T. Xiao, H. Guo, J.D. Morrey, N.E. Motter, K. Zhao, T.M. Block, A. Cuconati, *J Med Chem* **54**, 5660 (2011)
18. S.K. Pandey, A. Singh, A. Singh, *Eur J Med Chem* **44**, 1188 (2009)
19. A. Golisade, J. Wiesner, C. Herforth, H. Joma, A. Link, *Bioorg Med Chem* **10**, 769 (2002)
20. A. Domling, I. Ugi, *Angew Chem Int Ed* **39**, 3168 (2000)
21. A. Shaabani, A. Rahmati, A.H. Rezayan, H.R. Khavasi, *JICS* **8**, 24 (2011)
22. A. Shaabani, A. Rahmati, A.H. Rezayan, M. Darvishi, Z. Badri, A. Sarvari, *QSAR Comb Sci* **26**, 973 (2007)
23. V. Alagarsamy, V.R. Solomon, G. Vanikavitha, V. Paluchamy, M. Ravichandran, A. Arnaldsujin, A. Thangathirupathy, S. Amuth-alakshmi, R. Revathi, *Biol Pharm Bull* **25**, 1432 (2002)
24. M.M. Heravi, L. Ranjbar, F. Derikvand, B. Alimadadi, H.A. Oskooie, F.F. Bamoharram, *Mol Divers* **12**, 181 (2008)
25. R.G. Puligoundla, S. Karnakanti, R. Bantu, K. Nagaiah, S.B. Kondra, L. Nagarapu, *Tetrahedron Lett* **54**, 2480 (2013)
26. M.R. Mousavi, M.T. Maghsoodlou, N. Hazeri, S.M. Habibi-Khorassani, *JICS* **12**, 1419 (2015)
27. K. Kumari, D.S. Raghuvanshi, K.N. Sing, *Org Prep Proced Int* **44**, 460 (2012)
28. P.K. Sahu, *RSC Adv* **6**, 67651 (2016)
29. P.K. Sahu, *RSC Adv* **6**, 78409 (2016)
30. T. Wejrzanowski, R. Pielaszek, A. Opalin´ ska, H. Matysiak, W. Lojkowski, K.J. Kurzydowski, *Appl Surf Sci* **253**, 204 (2006)
31. R. Pielaszek, *J Appl Crystallogr* **1**, 43 (2003)
32. M.R. Mousavi, M.T. Maghsoodlou, *JICS* **12**, 743 (2015)
33. M.M. Heravi, F. Derikvand, L. Ranjbar, *Synth Commun* **40**, 677 (2010)

Publisher’s Note Springer Nature remains neutral with regard to jurisdictional claims in published maps and institutional affiliations.